THE JOURNAL OF PHYSICAL CHEMISTRY A

Article

Conformational Properties of Ethyl- and 2,2,2-Trifluoroethyl Thionitrites, (CXCHSNO, X = H and F)

Antonela Cánneva, Carlos Omar Della Védova, Norbert Werner Mitzel, and Mauricio Federico Erben

J. Phys. Chem. A, **Just Accepted Manuscript** • Publication Date (Web): 04 Sep 2014

Conformational Properties of Ethyl- and 2,2,2-Trifluoroethyl Thionitrites, (CX_3CH_2SNO, X = H and F)

Antonela Cánneva,[a] Carlos O. Della Védova[a,]*, Norbert W. Mitzel,[b] and Mauricio F. Erben [a,]*

[a] *CEQUINOR (UNLP-CONICET, CCT, La Plata), Departamento de Química, Facultad de Ciencias Exactas, Universidad Nacional de La Plata, CC962, La Plata (CP 1900), República Argentina*

[b]*Universität Bielefeld, Lehrstuhl für Anorganische Chemie und Strukturchemie, Centrum für Molekulare Materialien CM_2, Universitätsstraße 25, 33615 Bielefeld, Germany.*

[*] Corresponding authors: Tel/Fax: ++54-221-425-9485, E-mail: erben@quimica.unlp.edu.ar (MFE), carlosdv@quimica.unlp.edu.ar (CODV).

Abstract

The simple 2,2,2-trifluoroethyl thionitrite molecule, CF_3CH_2SNO, has been prepared in good yield for the first time using CF_3CH_2SH and NOCl in slight excess. The vapor pressure of the red-brown compound CF_3CH_2SNO follows, in the temperature range between 226 and 268 K, the equation $\log p = 12.0 - 3881/T$ (p/bar, T/K), and its extrapolated boiling point reaches 51 °C. Its structural and conformational properties have been compared with the ethyl thionitrite analogue, CH_3CH_2SNO. The FTIR spectra of the vapor of both thionitrites show the presence of bands with well-defined contours, allowing for a detailed conformational analysis and vibrational assignment on the basis of a normal coordinate analysis. The conformational space of both thionitrite derivatives has also been studied by using the DFT and MP2(full) level of theory with extended basis sets [6-311+G(2df) and cc-pVTZ]. The overall evaluation of the experimental and theoretical results suggests the existence of a mixture of two conformers at room temperature. The relative abundance of the most stable syn form (N=O double bond syn with respect to the C–S single bond) has been estimated to be ca. 79 and 75 % for CF_3CH_2SNO and CH_3CH_2SNO, respectively.

Keywords: S-nitrosothiol, Conformational analysis, IR Spectroscopy, Vibrational properties, Molecular structure.

1-Introduction

The first preparation of an *S*-nitrosophenylthiol species by reacting benzenethiol and nitrosyl chloride was reported more than a century ago by Tasker and Jones.[1] Different synthetic methods for thionitrites RSNO, are currently available in the chemical literature,[2-4] which includes outstanding reviews on its chemistry.[5] Mainly due to their thermal and photochemical instability, this family of compounds remained scarcely studied until recent times, when the formation and decomposition of RSNOs have been suggested as a mechanism for the storage and delivering of nitric oxide (NO) within the mammalian body.[6-9] Since then, a series of works have been reported in the literature, focusing on the study of fundamental properties of the simpler representatives, typically with R = alkyl or aryl groups.[10-14]

In this context, the first molecular structure experimentally determined for a thionitrite compound – *S*-nitroso-*N*-acetyl-D,L-penicillamine – was reported in 1978 by the Carnahan group.[15,16] The molecular structure of tri-phenyl thionitrite in the crystalline state determined by X-ray diffraction was reported in 1999 by Arulsami et al.[17] This structure shows an *anti* conformation [τ(CS-NO)=175.7°], with bond lengths of 1.792(5) and 1.177(6) Å for the S–N and N=O bonds, respectively.[17] On the other hand, the *syn* conformation [τ(CS-NO)= 0.7°] was observed in the crystal structure of *S*-nitrosocaptopril, which can deliver NO and captopril under physiological conditions, with S–N and N=O bond lengths of 1.766 and 1.206 Å, respectively.[18,19] Few other experimentally determined structures can be found in the literature.[19-21] In general it was assumed that – mainly due to sterical reasons – tertiary thionitrites prefer the *anti* conformation, whereas the *syn* form is adopted by primary derivatives. However, a delicate balance between both steric and electronic effects are known to affect the conformational behavior.[22] Moreover, for compounds containing a bond isomer with –

N=S=O unit it was also the case. The structure of PhNSO is planar and the introduction of two bulky ethyl groups in *ortho* positions does not change the transferable *syn* R–N=S=O configuration but rotate the –N=S=O group by 55.3° from a planar arrangement.[23]

For the "parent" HSNO species, benchmarking calculations suggest that the *anti* conformation is more stable than the syn one by 0.74 kcal/mol [CCSD(T)/AVQZ including corrections for core valence and scalar-relativistic and spin orbit effects][13,24] in very good agreement with recent calculations performed at the explicitly correlated coupled cluster approach (RCCSD(T)-F12) in connection with the cc-pVTZ-F12 basis set, that provides an accurate ΔE = 0.715 kcal/mol.[25]

Furthermore, on the basis of spectroscopic studies, it is well-known that the simplest alkylated derivative, methyl thionitrite (CH_3SNO), is present as a mixture of two conformers in the gas phase, with the *syn* conformer being the most abundant one.[26-29] By irradiating with visible light (between 485 and 590 nm) the mixture of both conformers isolated in a Ar matrix at 12 K, Müller and Huber determined a $\Delta G°_{298}$ = 1.33 ± 0.18 kcal/mol for the *syn*⇆*anti* equilibrium.[30] These conformational properties were also confirmed in the photodissociation dynamics of jet-cooled CH_3SNO using 355 nm polarized laser photolysis.[31]

It was reported for the related alkyl nitroso compounds, RONOs,[32,33] that the perfluorination of the alkyl group leads to a stabilization of the labile functional group,[28] but this seems not to be the case for RSNO compounds, in which the stability appears to decrease with increasing electron-withdrawing effect of R. To the best of our knowledge, the only known fluorinated thionitrite, CF_3SNO, was prepared by Mason in 1969 and its infrared and UV-vis spectra in the gas phase were interpreted in terms "*of a*

molecule of C_S symmetry, probably trans".[34] This preference for the *anti* conformer was recently confirmed by quantum chemical calculations at the B3P86/6-311+G(2df) and MP2/6-311+G(2df) level of approximations that yield an energy difference of ca. 1.5 and 0.9 kcal/mol, respectively.[22] CF_3SNO is the only known primary thionitrite with a marked preference for the *anti* form.

Prompted by these finding, we became interested in the conformational behavior of the ethyl derivatives. In particular, we want to establish if the presence of fluorine atoms asserts the conformational behavior through the so called "fluorine effect".[35] Since only few reports on the preparation[36] and fundamental properties[37] of CH_3CH_2SNO exist in literature, in the present work ethyl- and 2,2,2-trifluoro ethyl thionitrites, (CX_3CH_2SNO, X = H and F) have been synthesized and their gas phase infrared spectra fully analyzed accompanied by quantum-chemical calculations. It should be remarked that CF_3CH_2SNO is a novel thionitrite derivative, for which the preparation, proper isolation and characterization is provided within this contribution.

2-Experimental Section

The compounds were manipulated in a glass vacuum system equipped with PTFE stems (Young valves) and greased joints if it is necessary. All experiments were performed avoiding the presence of light. NOCl was prepared from NaCl and $NOHSO_4$ (Aldrich) following the reported method.[38] CH_3CH_2SNO was prepared from NOCl and CH_3CH_2SH (Aldrich, 95%).[1]

Synthesis of CF_3CH_2SNO: This molecule was prepared following the general method for the synthesis of RSNO derivatives reported by Tasker and Jones.[1] In general it

consists in the reaction of nitrosyl chloride with mercaptans, according the following equation:

$CF_3CH_2SH + NOCl \rightarrow CF_3CH_2SNO + HCl$

In a typical preparation, slightly more than the stoichiometric amount of NOCl was condensed onto 8 mmol of CF_3CH_2SH (Aldrich, 95%) maintained in vacuum in a reaction ampoule cooled in liquid nitrogen. The reaction tube was warmed briefly to melt the NOCl, re-cooled twice to –50 °C and maintained at that low temperature until a bright red liquid was obtained. The tube was warmed to ca. –20°C and the mixture purified by trap to trap distillation through traps held at –60, –90 and –196 °C. Pure CF_3CH_2SNO (ca. 7 mmol, 87 %) was obtained as a red-brown liquid in the –60 °C trap. HCl and minor quantities of NO were observed in the U-trap held at –196 °C.

Attempts to prepare CF_3CH_2SNO by the nitrite/thionitrite exchange method were also conducted.[39] In this case equimolar quantities of *tert*-butyl nitrite (Across, 95 %) and CF_3CH_2SH were co-condensed in a Carius tube. The reaction occurs as evidenced by the red coloration adopted by the reaction mixture at a temperature of –30 °C. However, the separation of the products mixture [presumably $(CH_3)_3COH$ and CF_3CH_2SNO] by using trap-to-trap distillation results much more difficult affecting the yield of the desired compound.

The new compound is a red-brown liquid at room temperature, and photosensitive in the presence of visible light. Signs of decomposition appear after 30 min of keeping a small sample at room temperature, as evidenced by the presence of NO in the infrared spectrum of the vapor. The vapor pressure of CF_3CH_2SNO follows, in the temperature range between 226 and 268 K, the equation $\log p = 12.0 - 3881/T$ (p/bar, T/K), and the boiling point can be extrapolated to be 51 °C.

The ^{1}H NMR spectrum only shows a quartet signal located at δ = 3.43 ppm, $^{3}J_{(F,H)}$= 9.8 Hz, that corresponds to the CH_2- group of the molecule. In the ^{19}F NMR spectrum one triplet located at δ = –65.9 ppm can be observed with the same $^{3}J_{(F,H)}$ coupling. In addition, the ^{13}C NMR spectrum of the fluorinated title compound shows two quartet signals at δ = 127.1 ($^{1}J_{(F,C)}$ = 277 Hz) and 43.4 ($^{2}J_{(F,C)}$ = 31 Hz) ppm, assigned to the carbon atoms of the CF_3 and CH_2 groups, respectively. These values are in sound agreement with those reported for the related $(CF_3CH_2S)_4Sn$ compound.[40] Additional evidence for the identity of CF_3CH_2SNO can be gained from the analysis of its gas IR spectrum, as discussed below.

Vibrational Spectroscopy: Gas-phase infrared spectra were recorded with a resolution of 1 cm^{-1} in the range 4000–400 cm^{-1} with a Bruker IFS 66v FTIR instrument.

Computational Methods: All quantum-chemical calculations were performed with the Gaussian 03 program package.[41] As suggested by Marazzi et al.[22] MP2 and B3P86 methods[42] and gradient techniques were used for the geometry optimizations and vibrational properties, together with standard basis sets up to the Pople-type 6-311+G(2df) basis set that includes diffuse and polarization functions, and Dunning´s correlation-consistent basis set of valence triple-ζ (cc-pVTZ). For comparison, other classic hybrid functionals[43] (B3LYP[44] and B3PW91) were also applied. Optimization geometry and frequencies were performed with Opt = VeryTight and Integral (Grid = UltraFine) option, respectively. For the normal coordinate analysis, transformations of the *ab initio* Cartesian harmonic force constants to the molecule-fixed internal coordinates system were performed, as described by Hedberg and Mills and implemented in the ASYM40 program.[45] This procedure evaluates the potential energy distribution (PED) associated with each normal vibrational mode under the harmonic assumption. The internal and symmetry coordinates used to perform the normal

coordinate analysis are defined in Figure S1 and Table S1, in the Supporting Information.

3-Results and discussion

3.1-Conformational analysis

The potential energy curves for the internal rotation around C–S and S–N bonds were obtained by structure optimization at fixed dihedral angles from 0 to 180° in steps of 10°, at the B3P86/6-311+G(2df) level of approximation, for both CH_3CH_2SNO and CF_3CH_2SNO compounds. As shown in Figure 1 (left), the potential energy curves for rotation around the S–N bond are similar, with two minima at 0 and 180°. In both cases, the most stable form corresponds to the *syn* conformation (C–S single and N=O double bonds in mutual synperiplanar orientation). The *anti* conformer is observed higher in energy by around 0.7 kcal/mol, with C–S single and N=O double bonds in antiperiplanar conformation. The curves are nearly symmetrical with respect to a local maximum at δ(CS-NO) = 90°, corresponding to a torsional transition state with a computed energy barrier to internal rotation of 15.2 kcal/mol (CH_3CH_2SNO) and 14.1 kcal/mol (CF_3CH_2SNO). The computed [B3P86/6-311+G(2df)] geometries for the transition states of CF_3CH_2SNO and CH_3CH_2SNO give similar δ(CS-NO) values (82.5 and 82.9º, respectively). The S–N bond is elongated with respect to the minimum geometry (see Section 3.2), reaching values of 2.007 and 1.942 Å, while the N=O bond is reinforced, with *r*(N=O) bond lengths of 1.145 and 1.158 Å for the transition states of CF_3CH_2SNO and CH_3CH_2SNO, respectively. Thus, strong electronic reorganizations occur upon S–N bond rotation, doubtless affecting the high of the rotational barrier.

Figure 1 (right) shows the potential energy curves calculated for the internal rotation around the C–S bond of CF_3CH_2SNO and CH_3CH_2SNO, corresponding to the formal rotation of the 2,2,2-trifluoroethyl and ethyl groups with respect to the –SNO group, respectively. For both compounds, the global minimum corresponds to a structure with gauche conformation, with δ(CC–SN) ≈ 110° for CF_3CH_2SNO, while the corresponding minimum for the ethyl derivative lies in a flat portion of the potential energy curve. It is important to notice that both the *syn* and *anti* conformations around the C–S bond [δ(CC–SN) = 180°] are located in a local maxima in the potential energy curve. Further harmonic frequency calculations allowed to assign the anti form as a rotational transition state connecting two energetically equivalent forms of the *gauche* rotamer (±-*gauche*). The computed barriers are 1.0 and 2.1 kcal/mol, higher for the 2,2,2-trifluoroethyl derivative, suggesting the influence at least of steric factors for the bulky CF_3CH_2– moiety.

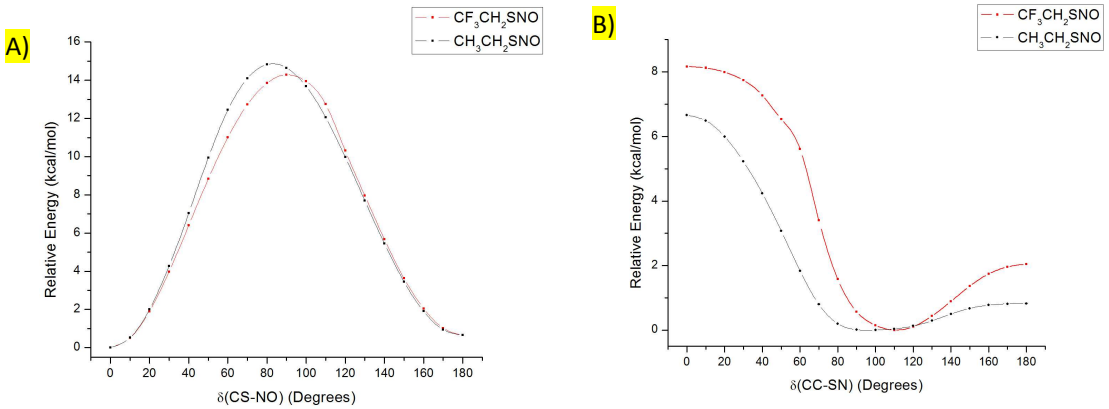

Figure 1. Calculated [B3P86/6-311+G(2df)] potential energy function for internal rotation around S–N (A) and C–S (B) single bonds in CF_3CH_2SNO (red line) and CH_3CH_2SNO (black line).

Full geometry optimizations and frequency calculations for each of the most stable structures have been performed by using DFT and MP2(full) methods with relative large basis sets [6-311+G(2df) and cc-pVTZ]. Following Marazzi et al.[22] three hybrid functional (B3P86, B3LYP and B3PW91) have been applied. The optimized structure of the *syn* and *anti* conformers of CF_3CH_2SNO and CH_3CH_2SNO are shown in Figure 2. The results obtained at all tested level of approximations are in accordance with the fact that the *syn* form is more stable than the *anti* one. The computed energy difference (corrected by zero point energy) and Gibbs free energy differences (in kcal/mol) between the *anti* and *syn* forms are listed in Table 1. It can be observed that the cc-pVTZ polarized Dunning's type basis set systematically gives slightly higher differences in energy values than the Pople-type basis set 6-311+G(2df) with polarization and diffuse functions. Difference energy values (ΔE^0) computed with the same method of approximations with less extended basis sets are given in Table S2 (Supporting Information). For both compounds, the ΔE^0 computed with the 6-31G(d) is much larger than that obtained with more extended basis sets.

As was previously observed for other thioinitrites,[22] the explicit inclusion of electron correlation in the MP2 method computes higher energy differences than those obtained by using DFT methods.

Accordingly to the Boltzmann distribution and by taking into consideration the calculated ΔG^0 values at the MP2(full)/cc-pVTZ level of approximation, a relative

abundance of roughly 21 and 26 % of the less stable *anti* form is expected to be present at room temperature in the vapor of CF_3CH_2SNO and CH_3CH_2SNO, respectively.

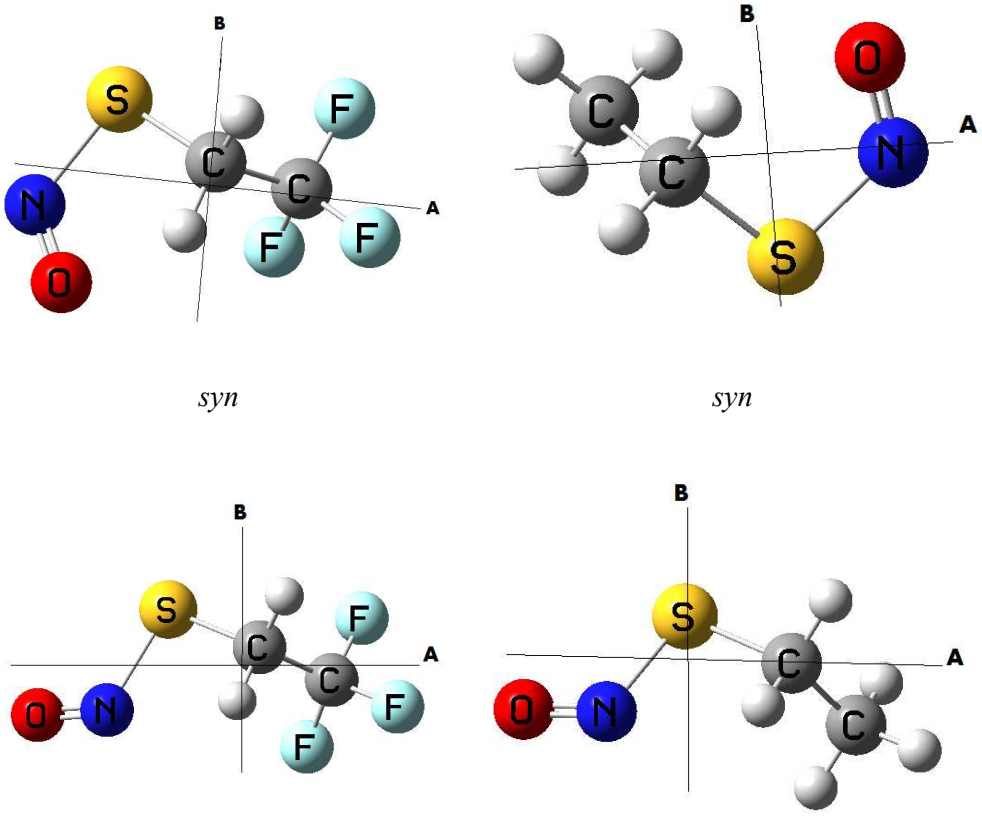

Figure 2. Molecular models for the two main conformers of CF_3CH_2SNO (left) and CH_3CH_2SNO (right). Principal axes of inertia are displayed (the *C*-axis is perpendicular to the plane formed by the *A*- and *B*-axes).

Table 1. Calculated relative energy (corrected by zero-point energy) and Gibbs free energy differences (in kcal/mol) for CX_3CH_2SNO (X = F and H) and concentration of the most stable *syn* forms.

Level of approximation		CF_3CH_2SNO			CH_3CH_2SNO		
		$\Delta E°$	$\Delta G°$	%	$\Delta E°$	$\Delta G°$	%
B3P86	**6-311+G(2df)**	0.65	0.52	71	0.68	0.82	80
	cc-pVTZ	0.75	0.65	75	0.79	0.92	83
B3LYP	**6-311+G(2df)**	0.37	0.25	60	0.42	0.44	68
	cc-pVTZ	0.52	0.43	68	0.58	0.66	75
B3PW91	**6-311+G(2df)**	0.46	0.34	64	0.51	0.64	75
	cc-pVTZ	0.56	0.46	69	0.61	0.71	77
MP2(full)	**6-311+G(2df)**	0.86	0.60	74	1.04	0.39	66
	cc-pVTZ	1.02	0.78	79	1.24	0.63	74

3.2- Molecular structure

It was reported[46] that different quantum chemical methods with an appropriate large basis set generally give optimized structures of RSNOs, in close agreement with each other. The B3P86/6-311+G(2df) and MP2(full)/cc-pVTZ computed geometrical parameters for optimized molecular structures for *syn* and *anti* conformers of CH_3CH_2SNO and CF_3CH_2SNO are given in Table 2. For completeness, the results obtained for the most stable syn conformer, computed at the same methods with the less extended 6-31G(d) and 6-311+G(d) basis sets are given in Table S3 in the Supporting Information.

Table 2. Computed geometrical parameters (distances in Å, angles in deg) for *syn* and *anti* conformers of CX_3CH_2SNO (X = H and F) at different levels of approximation.

Parameter	CF_3CH_2SNO	CH_3CH_2SNO

	B3P86 6-311+G(2df)		MP2(full) cc-pVTZ		B3P86 6-311+G(2df)		MP2(full) cc-pVTZ	
	syn	*anti*	*syn*	*anti*	*syn*	*anti*	*syn*	*anti*
r(N=O)	1.174	1.168	1.182	1.178	1.183	1.178	1.202	1.194
r(S–N)	1.823	1.835	1.850	1.853	1.792	1.803	1.775	1.796
r(C–S)	1.787	1.792	1.780	1.787	1.799	1.805	1.794	1.800
r(C–C)	1.510	1.511	1.501	1.502	1.518	1.516	1.514	1.513
∠(SNO)	117.5	116.4	116.3	116.1	117.5	116.7	116.3	116.0
∠(NSC)	101.3	93.5	99.4	91.8	102.5	95.2	100.8	93.7
∠(CCS)	113.9	113.7	113.4	113.3	113.8	113.6	112.8	113.1
∠(SCH)	106.8	108.6	108.7	108.7	105.9	106.0	106.1	106.0
∠(CCH)	108.5	108.5	108.3	108.3	111.5	111.6	111.6	111.6
∠(HCH)	109.0	108.9	109.4	109.4	107.7	107.6	108.3	108.1
∠(XCC)	111.3	111.3	111.2	111.2	110.9	110.9	110.5	110.5
∠(XCX)	107.5	107.6	107.7	107.7	108.0	108.0	108.4	108.4
δ(CS-NO)	0.4	179.4	0.4	178.0	0.3	179.0	0.5	177.9
δ(NS-CC)	110.1	107.9	98.9	102.5	97.9	107.7	83.6	97.8
δ(SC-CX)	179.3	179.3	178.6	179.8	179.8	179.0	179.0	179.4

The computed [MP2(full)/cc-pVTZ] values for *r*(N=O) and *r*(S–N) bond length of the *syn* form of CH_3CH_2SNO, i.e. 1.202 and 1.775 Å, respectively, are in reasonable agreement with those previously reported (1.188 and 1.792 Å) at the QCISD/6-311G(df,p) level of approximation.[46] The N=O bond is longer for the *syn* conformers of both compounds here studied. On the other hand, and in agreement with previous

results[22] for primary RSNO compounds, the S–N bond is longer in the *anti* than in *syn* conformer. As suggested by Timerghazin et al.[11,13] the repulsion of lone pairs of electrons between sulfur and oxygen may be responsible for the longer N=O bonds found in *anti* RSNO compounds.

Interestingly, the larger difference in the geometrical parameters between both conformers is evidenced by the CSN bond angle for both CH_3CH_2SNO and CF_3CH_2SNO compounds. In effect, the MP2(full)-cc-pVTZ computed values for ∠(CSN) are 91.8 and 93.7 degrees for the *anti* rotamer of CH_3CH_2SNO and CF_3CH_2SNO, respectively, which are around 8° smaller than that in the *syn* form. This tendency can also be rationalized by steric effects acting in the *syn* form, mainly due to the repulsion of both lone pairs of electrons formally located at the sulfur and oxygen atoms.

When the computed geometrical parameters are compared between CF_3CH_2SNO and CH_3CH_2SNO, important differences are found, especially in the thionitrite group. Both methods reproduce the same trend, and the MP2(full)/cc-pVTZ will be further considered. In effect, the N=O bond is shorter in the fluorinated compound by 0.02 Å, while the S–N bond is longer by 0.075 Å. In agreement with recent results on RSNO compounds,[46] the S–N bond in CX_3CH_2SNO (X = H and F) should be considered as a single bond, without double bond character, as was early assumed.[47] Moreover, such a weaker S–N bond for CF_3CH_2SNO may be a factor to explain the high instability experimentally observed for this compound.

3.3-Vibrational analysis

Figures 3 and 4 show the FTIR spectra of gaseous CH_3CH_2SNO and CF_3CH_2SNO, respectively. Frequency calculations at the MP2(full)/cc-pVTZ level of approximation have been performed to assist the analyses of the experimental results. A tentative assignment of the observed bands was carried out based on the calculated displacement vectors for the fundamentals, as well on comparison with the spectra of related molecules, particularly CX_3SNO (X = F[34] and H[26-29]). The previous vibrational analysis reported for the CH_3CH_2SNO species has been especially considered in the light of the new available data.[37] Furthermore, the PED associated with each normal vibrational mode has been calculated under the harmonic assumption. From PED analysis, it becomes clear that, as expected, many vibrations have a high degree of mixture. Therefore, tentative assignments for characteristic and intense spectral features in the vibrational spectra of the molecules are discussed. Tables 3 and 4 list the vibrational results for CH_3CH_2SNO and CF_3CH_2SNO, respectively.

It is well-known that the detailed analysis of band contours in infrared spectra can provide valuable information regarding the gas-phase structure of rotamers.[48-50] The experimentally observed band contours for CF_3CH_2SNO and CH_3CH_2SNO are also listed in Tables 3 and 4. Calculated rotational constants (cm^{-1}) and molecular parameters, together with the estimated separation between P and R branches [$\Delta\nu$(PR) values, in cm^{-1}] – as obtained following the classical method of Seth-Paul[51] – are collected in Table 5. Both molecules can be classified as prolate asymmetric rotors. It should be noted that since relative high ρ^* values ($\rho^* > 1$) are computed, the PQQR band structure expected for B-type contours passes into a band structure with only two maxima (PQ and QR) branches.

CH_3CH_2SNO

A tentative assignment for infrared spectrum of ethyl thionitrite, CH_3CH_2SNO, was early reported by Philippe and Moore,[37] by assuming that alkyl thionitrite molecules belong to the C_S point group of symmetry. However, with the help of quantum-chemical calculations, it was clearly demonstrated that CH_3CH_2SNO adopts C_1 symmetry.[46] The calculated [MP2(full)/cc-pVTZ] symmetry parameter (κ = –0.42) for *syn* CH_3CH_2SNO with C_1 symmetry indicates that the molecule can also be classified as prolate asymmetrical top. When compared with the 2,2,2-trifluoro derivative, higher separations between P- and R- branches are calculated, in agreement with the lower mass of the hydrogen with respect to the fluorine atoms. The $\Delta\nu$(PR) expected for the most stable *syn* conformer amounts 16.4, 12.6 and 24.6 cm^{-1} of the A, B and C type-bands, respectively.

The spectrum of CH_3CH_2SNO clearly shows bands associated with the CH_3 antisymmetric modes of vibration at 2988 and 2981 cm^{-1} and the totally symmetric vibration of the CH_3 group at 2888 cm^{-1}. The 2945 cm^{-1} band with a definite PQR structure can be assigned to C–H antisymmetric stretching mode of the $–CH_2–$ group.

The stretching mode ν(N=O) and its first overtone can be used to solve one of the fundamental questions in the present study testing the conformational equilibrium of this and the partially fluorinated species. This normal mode of vibration can be assigned to a strong and broad band with an approximated B contour and maxima at 1538 and 1530 cm^{-1}, in perfect agreement with the previously reported value of 1534 cm^{-1}.[37] Its B-type envelope can be originated from the quasi parallelism of this oscillator in relation with the B principal moment of inertia (Figure 2). It is interesting to note that, superimposed to this band at higher energies and centered at 1559 cm^{-1} an A-type band is observed in the gas infrared spectrum (see Figure 3, inset). It is reasonable to assume that this absorption corresponds to the N=O stretching vibration of the *anti* form, in

agreement with the relative orientation of this oscillator with respect to the principal moments of inertia depicted in the Figure 2. The branch separations for these A and B bands also agree quite well with the calculated results listed in Table 5. The assignment related to the N=O stretching vibrations to the two rotamers is confirmed by the evaluation of their N=O overtones. Centered in 3083 and 3034 cm^{-1} two weak bands with B and A contours, respectively, can be observed in the FTIR spectrum of the gaseous sample. These bands can be straightforward assigned to the first N=O stretching vibration overtones belonging to both the *anti* and the *syn* conformation, respectively, taken into account their contours, relative intensities and the duplication of the wavenumbers difference with relation to their two fundamental modes (49 cm^{-1} in case of the first overtones and 25 cm^{-1} for the N=O fundamental mode of vibration). The MP2(full)/cc-pVTZ computed frequency values for the ν(N=O) fundamentals are too low (1524 and 1492 cm^{-1} for the *anti* and *syn* conformers, respectively).

In agreement with the previously reported vibrational assignment,[37] the bands at 1464, 1457 and 1384 cm^{-1} are tentatively associated with the deformation motions of the CH_3 and CH_2 groups.

As recognized by Philippe and Moore,[37] the assignment of vibrations such as the C–S and N–S stretching and C–H and S–N=O deformation modes is not straightforward. Therefore and based on the results derived from both, the band contour analysis and quantum chemical calculations, a tentative assignment is presented in Table 3. The weak absorptions at 1045 cm^{-1} and the B-type band centered at 974 cm^{-1} could originate from the ν(C–C) and $\rho_{ac}(CH_3)$ fundamental modes of vibration. More important, on the basis of the potential energy distribution analysis, the band centered at 693 cm^{-1} is now assigned to the ν(C–S) stretching vibration. The AB-type band observed with medium intensity centered at 629 cm^{-1} is generated by the δ(SNO)

motion, in good agreement with the computed value (648 cm^{-1}). Our MP2(full)/cc-pVTZ results suggest that the ν(S–N) stretching mode contributes to a vibration appearing near 400 cm^{-1} (the computed value for the *syn* form is 398 cm^{-1}). As observed in Figure 3, an incomplete band rises below the limit of our spectrophotometer

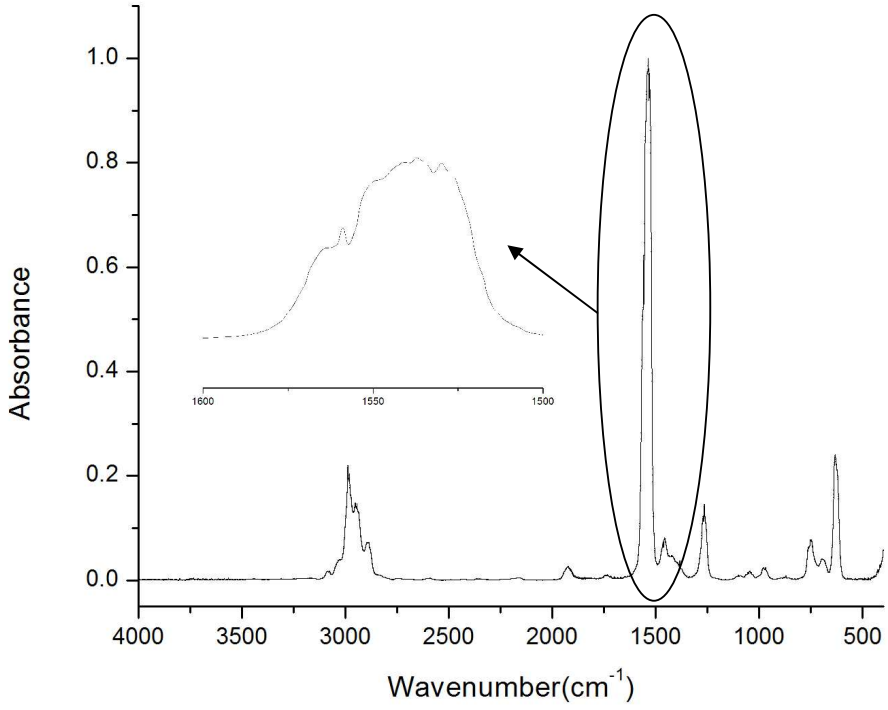

Figure 3. Gas phase FTIR of CH_3CH_2SNO at 11 mbar (glass cell, 10 cm optical path length, KBr windows, 2 mm thick). The inset shows the enlargement of the ν(N=O) absorption band.

Table 3: Observed and Calculated [MP2(full)/cc-pVTZ] Vibrational Data (cm^{-1}) for CH_3CH_2SNO

IR (gas)[a]	Band contour. (Δν(PR))	MP2(full)/cc-pVTZ[b]		Tentative assignment
		syn	*anti*	
3089 QR (vw) 3078 QP (vw)	B (11)			2*ν(N=O) anti
3041 R 3034 Q (vw) 3029 P	A (12)			2*ν(N=O) syn
2988 (vw)		3187(4)	3183 (5)	$\nu_{as}CH_3(90)+\nu_{as}(CH_2)(10)$
2981 (vw)		3172(6)	3168 (7)	$\nu_{as}CH_3(100)$
2953 R 2945 Q(vw) 2938 P	A (15)	3155(0.3)	3154 (0.4)	$\nu_{as}(CH_2)(80)+ \nu_s(CH_3)(10)+\nu_s(CH_2)(10)$
		3100(4)	3107 (4)	$\nu_s(CH_2)(70)+\nu_s(CH_3)(20)+\nu_{as}(CH_2)(10)$
2888 (vw)		3099(7)	3095 (8)	$\nu_s(CH_3)(80)+\nu_s(CH_2)(20)$
2167(vw)				ν(N=O)+δ(SNO)
1923(vw)				ν(N=O)+ ν(S-N)
1564 R 1559 Q (vs) 1550 P	A (14)		1524 (100)	$\nu(N=O)(80)+\delta_{as}(CH_2)(20)$ (anti)
1538 QR (s) 1530 QP (s)	B (8)	1492(100)		$\nu(N=O)(65)+\rho(CH_2)(20)$ (syn)
1464 (vw)		1457(27)	1478 (2)	$\rho(CH_2)(80)+ \nu(N=O)(20)$
		1525(2)	1522 (29)	$\delta_{as}(CH_3)(100)$

1457 (vw)		1521(0.5)	1520 (37)	$\delta_{as}(CH_3)(100)$
		1421(4)	1423 (2)	$\delta_{s}(CH_3)(100)$
1384 (vw)		1307(10)	1315 (7)	$\rho_{as}(CH_2)(85)+ \rho_{s}(CH_2)(15)$
1272 R 1265 Q (vw) 1259 P	AC (23)	1294(1)	1299 (3)	$\rho_{s}(CH_2)(80)+ \rho_{as}(CH_3)(20)$
1045 (vw)		1096(1)	1102 (0.1)	ν(C-C)(60)+ $\rho_{as}(CH_3)(40)$
		1062(1)	1067 (3)	$\rho_{as}(CH_3)(50) + \rho_{s}(CH_2)(35)+ \rho(CH_2)(15)$
981 (vw) QR 971 (vw) QP	B (10)	1007(2)	1011 (3)	$\rho_{as}(CH_3)(45)+ \nu$(C-C)(45)+ $\rho_{as}(CH_2)(10)$
752 (vw)		768(21)	761 (5)	$\rho(CH_2)(40)+\delta$(SNO)(30)+ $\rho_{as}(CH_3)(30)$
693 (vw)		713(1)	721 (5)	ν(C-S)(80) + $\rho(CH_2)$ (20)
635 (w) R 623 (w) P	AB (12)	648(33)	658 (66)	δ(SNO)(60) + $\rho(CH_2)(25)$ + ν(S-N)(15) + ν(C-S)(10)
		398(68)	394 (41)	ν(S-N)(100)
		371(4)	327 (7)	δ(CCS)(55)+ τ (CS-NO)(45)
		305(3)	292 (6)	τ(HC-CS)(55)+δ(CSN)(45)
		248(0.2)	211 (0.1)	τ(CS-NO)(65)+δ(CCS)(35)
		210(3)	194 (8)	τ(CS-NO)(50)+δ(CSN)(50)
		91(0.4)	38 (0.1)	τ(CC-SN)(100)

[a] Band Intensity: vs = very strong, s = strong, m = medium, w = weak, vw = very weak. [b] In parentheses relative band strengths for the two most stable forms, IR intensities (100% = 204 km/mol for *syn-gauche* form and 100% = 220 km/mol for the *anti* form). [C] Unless indicated, band assignment and PED values correspond to the most stable conformer, only contribution larger than 10% are given.

CF_3CH_2SNO

The calculated [MP2(full)/cc-pVTZ] symmetry parameter (κ = -0.84) for *syn* CF_3CH_2SNO indicates that the molecule can be classified as prolate asymmetrical top. The expected separation between P- and R- branches are 9.8, 7.8 y 14.6 cm^{-1} of the A, B and C type-bands, respectively. Slightly minor separations are expected for the *anti* conformer, as also listed in Table 5. However, rather distinctive the A, B and C band contours can be originated from both *syn* and *anti* conformers, depending on the relative orientation of the transition dipole moments with respect to the *A*, *B*, and *C* principal axis of inertia.

As earlier mentioned the gas phase IR spectrum of RSNOs is characterized by a strong absorption appearing in the 1700–1500 cm^{-1} range, that correspond to the ν(N=O) stretching mode.[37] This mode is quite sensitive to the nature of the R substituent. For CH_3SNO the corresponding values are 1548 and 1527 cm^{-1} for the *anti* and *syn* forms, respectively, as determined from matrix isolation experiments.[30] For the related CF_3SNO species in its more stable anti conformation, this mode is observed at 1700 and 1660 cm^{-1} in the infrared spectra of the solid and vapor, respectively.[34]

In line with this tendency, the N=O stretching vibrations of the *anti*- and *syn*-CF_3CH_2SNO are observed at higher wavenumbers than that of the analogous rotamers of CH_3CH_2SNO. Thus, a well-defined absorption with PQR structure at 1605 cm^{-1} is assigned to the N=O stretching vibration of the anti form taken into account the envelope and the comparison with the computed results (Table 4). At lower wavenumbers another absorption with a B-type contour centered at 1580 cm^{-1} can be assigned to the N=O stretching vibration of the more abundant *syn* rotamer. As in case of the parent methylated molecule the evaluation of the N=O overtone region is

indicative to establish the conformational behavior of the molecule. As in case of the former analyzed species and centered at 3173 (B-contour) and 3127 cm^{-1} (A-contour) two bands can be assigned to the first N=O overtone of both the *anti* and *syn* conformers, respectively, in view of their envelopes, band separation, relative intensity and the difference between them as compared with N=O normal mode of vibration (46 and 25 cm^{-1}, respectively).

The ν(C–F) stretching vibrations for CF_3SNO were assigned to three strong absorptions observed in the infrared spectrum at 1140 (A″), 1100 (A′) and the totally symmetric at 1083 cm^{-1}.[34] In the CF_3CH_2SNO spectrum, the strong absorptions centered at 1148 cm^{-1} (with PQR structure) and the B-band at 1093 cm^{-1} are assigned to these C–F antisymmetric stretching modes.

It is rather difficult to assign with confidence the ν(C–S) and ν(S–N) stretching vibrations in CF_3CH_2SNO, since both vibrational modes are sensitive to substitution at the sulfur. For example, extreme differences are reported for the C–S stretching vibration where the ν(C–S) normal mode appears at 731 cm^{-1} in CH_3SNO and decreases upon fluorine substitution to 442 cm^{-1} in CF_3SNO.[34] On the other hand, the ν(S–N) mode is found at 759 cm^{-1} in CF_3SNO,[34] a higher value than for CH_3SNO, at 649 cm^{-1}. In qualitative agreement with these features, a band of medium intensity with an A-contour centered at 781 cm^{-1} is observed in the infrared spectrum of CF_3CH_2SNO, which is tentatively assigned to the ν(C–S) stretching, while the ν(S–N) is computed at 295 cm^{-1}, below the cut-off of the KBr windows used in the measurements and the limit of our spectrometer.

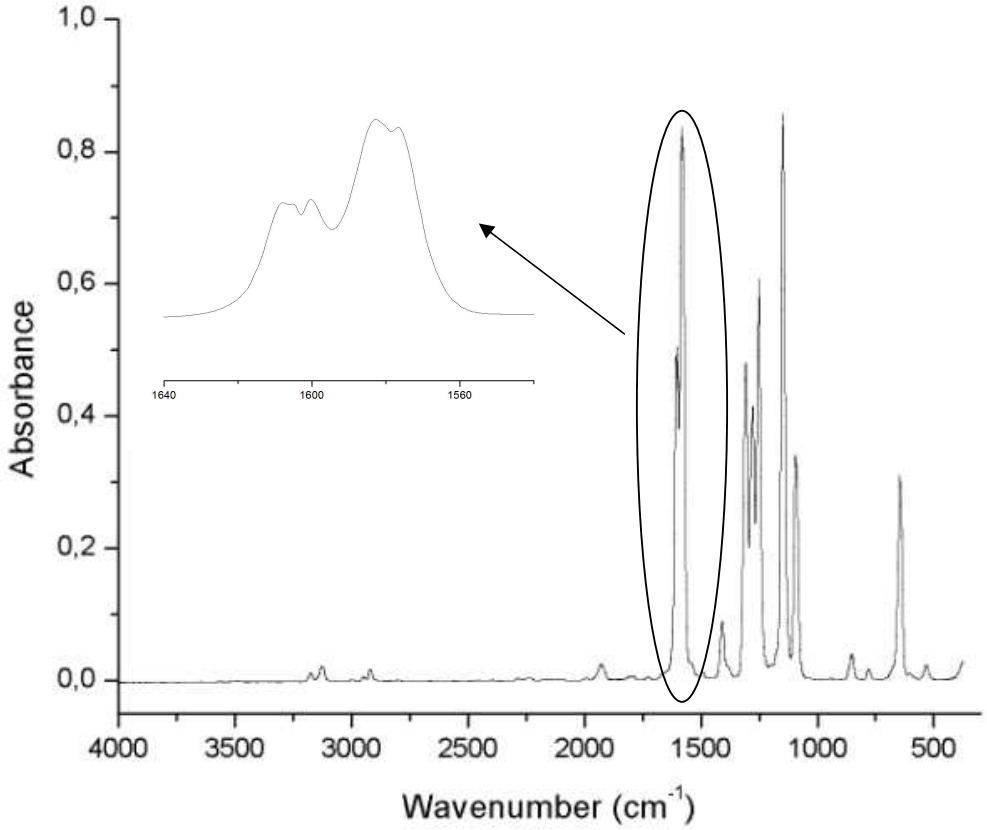

Figure 4. Gas phase FTIR at 10.0 mbar of CF_3CH_2SNO (glass cell, 10 cm optical path length, KBr windows, 2 mm thick). The inset shows the enlargement of the ν(N=O) absorption bands.

Table 4. Observed and Calculated [MP2(full)/cc-pVTZ] Vibrational Data (cm^{-1}) for CF_3CH_2SNO

IR (gas)[a]	Band contour. (Δν(PR))	MP2(full)/cc-pVTZ[b]		Tentative assignment (PED)
		syn	*anti*	
3176 QR (vw) 3169 QP (vw)	B (7)			2*ν(N=O) anti
3132 R 3127 Q (vw) 3123 P	A(9)			2*ν(N=O) syn
3000 QR (vw) 2993 QP (vw)	B (7)	3187 (0.7)	3188 (0.2)	$\nu_{as}(CH_2)(70) + \nu_s(CH_2)(30)$
2951 R 2947 Q (vw) 2942 P	A (9)	3079 (3)	3115 (2)	$\nu_s(CH_2)(70) + \nu_{as}(CH_2)(30)$
2921 (vw)				?

2285 (vw)				2* $\delta_s(CH_2)$
2234 (vw)				$\delta_{as}(CH_2) + \delta_{as}(CH_2)$
1930 (vw)				$\nu(N=O) + \delta(SNO)$
1608 R 1605 Q (s) 1600 P	A (8)		1586 (100)	$\nu(N=O)$ (95) (anti)
1583 QR (vs) 1577 QP (vs)	B (6)	1572 (100)		$\nu(N=O)$ (100) (syn)
1408 (vw)		1452 (12)	1461 (6)	$\delta(CH_2)(80) + \nu(C–C)(10) + \delta_{as}(CH_2)(10)$
1312 R 1308 Q (s) 1304 P	A (8)	1358 (46)	1367 (32)	$\nu(C–C)(40) + \delta_{as}(CH_2)(25) + \nu_s(CF_3)(20) + \delta_s(CF_3)(15)$
1283 QR (s) 1277 PQ (s)	B (6)	1325 (41)	1326 (30)	$\rho(CH_2)(45) + \nu_{as}(CF_3)(45) + \delta_{as}(CF_3)$ (10)

1254 R 1251 Q (s) 1246 P	A (8)	1287 (38)	1291 (28)	$\delta_{as}(CH_2)(45) + \nu_{as}(CF_3)(35) + \delta_s(CF_3)(10) + \nu_s(CF_3)(10)$
1151 R 1148 Q (vs) 1144 P	A (7)	1184 (65)	1186 (52)	$\nu_{as}(CF_3)(65) + \delta_{as}(CH_2)(25) + \delta_{as}(CF_3)(10)$
1096 QR (m) 1090 QP (m)	B (6)	1131 (32)	1132 (17)	$\nu_{as}(CF_3)(50) + \rho(CH_2)(50)$
855 QR (w) 850 QP (w)	B (5)	884 (2)	886 (4)	$\nu_s(CF_3)(50) + \nu(C\text{-}C)(30) + \nu(C\text{-}S)(20)$
		867 (0.9)	879 (3)	$\rho(CH_2)(75) + \nu_{as}(CF_3)(15) + \delta(CSN)\ (10)$
784 R 781 Q (vw) 776 P	A (8)	813 (1)	816 (0.6)	$\nu(C\text{–}S)(60) + \nu_s(CF_3)(15) + \delta(CCS)\ (15) + \rho_s(CF_3)(10)$

		673 (24)	665 (28)	δ(S–NO)(90) + ν(S–N)(10)
648 QR (m) 643 QP (m)	B (5)	659 (6)	657 (7)	$\delta_s(CF_3)$(70) + δ(CCS)(10) + ν(CC)(10) + $\nu s(CF_3)$ (10)
534 QR (vw) 529 QP (vw)	B (5)	546 (1)	545 (1.4)	$\delta_{as}(CF_3)$(70) + $\delta_s(CF_3)$(10) + $\delta_{as}(CF_3)$(10) + ν(C–S)(10)
		541 (2)	544 (0.2)	$\delta_{as}(CF_3)$(90) + $\rho(CH_2)$(10)
		390 (1)	395 (7)	$\rho_{as}(CF_3)$(45) + $\rho(CH_2)$(15) + $\rho_s(CF_3)$(15) + δ(CSN)(15) + $\delta_{as}(CF_3)$(10)
		359 (1)	362 (0.7)	$\rho_{as}(CF_3)$(35) + $\rho_s(CF_3)$(35) + $\delta_{as}(CF_3)$(15) + ν(C–S)(15)
		294 (38)	293 (23)	ν(S–N)(70) + ν(N=O)(15) + τ (CSNO)(15)
		269 (20)	223 (0.2)	ν(S–N)(50) + τ(CSNO)(40) + ν(N=O)(10)
		235 (4)	208 (8)	δ(CSN)(75) + $\rho_{as}(CF_3)$(15) + ν(S–N)(10)
		170 (0.5)	179 (1)	δ(CCS)(65) + $\rho_{as}(CF_3)$(25) + ν(S–N)(10)
		73 (<0.1)	71 (0.2)	τ(CF_3)(85) + δ(CSN)(15)
		51 (0.2)	42 (0.1)	τ (CCSN)

[a] Band Intensity: vs = very strong, s = strong, m = medium, w = weak, vw = very weak. [b] In parentheses relative band strengths for the two most stable forms, IR intensities (100% = 324 km/mol for *syn-gauche* form and 100 %= 445 km/mol for the *anti* form). [C] PED values correspond to the most stable conformer, only contribution larger than 10% are given.

Table 5. Rotational constants (cm^{-1}), asymmetry parameters and P-R branch separation (cm^{-1}) calculated at the MP2(full)/cc-pVTZ for CX_3CH_2SNO (X= H and F)

		A	*B*	*C*	*κ*	*ρ**	*β*	*S(β)*	**Δ*ν*(PR)** [b]		
									***A*(‖)**	***B*(⊥)**	***C*(⊥)**
CH_3CH_2SNO	***syn***	0.1968	0.1157	0.0825	-0.420	0.988	0.701	1.33	16.44	12.62	24.65
	anti	0.3244	0.0753	0.0677	-0.437	3.411	3.552	1.18	12.86	10.86	19.29
CF_3CH_2SNO	***syn***	0.1016	0.0395	0.0341	-0.840	1.708	1.572	1.265	9.8	7.8	14.8
	anti	0.1215	0.0317	0.0296	-0.953	2.897	2.829	1.206	8.5	7.1	12.8

[a] Asymmetry parameters: κ= (2B–A–C)/(A–C), ρ*= (A–C)/B, β+1 = A/B (prolate top), log S(β)= 0.712/(β+4)[1.13]. [b] P-R band separation are defined and calculated according to Seth-Paul.[51]

4-Conclusion

A proper method for the preparation and isolation of pure CF_3CH_2SNO has been achieved. The conformational, structural and vibrational properties have determined on the basis of a detailed analysis of the infrared spectrum augmented with the band envelope evaluation. The overall evaluation of the experimental and theoretical results suggests the existence of a mixture of two conformers of CF_3CH_2SNO at room temperature in the gas phase, the *syn* form (N=O double bond adopting a *syn* orientation with respect to the S–C single bond) being preferred over the *anti* one [MP2(full)/cc-pVTZ computed $\Delta E^0 \approx 1$ kcal/mol]. A similar conformational behavior was determined for the related CH_3CH_2SNO species.

The ν(N=O) stretching band is one of the most intense absorptions observed in the infrared spectra of RSNO compounds and –as demonstrated here– it is sensitive to the conformation around the S–N bond. Its first overtone can be subsequently detected adding information to resolve the conformational problem. In order to better determine the frequency values expected for the *syn* and *anti* conformers of the studied molecules, quantum-chemical calculations at different level of approximations have been further performed, the results being collected in Table 6. When MP2 and DFT methods are compared, strong variations can be found in the computed values, the DFT frequencies are found systematically at higher values (ca. 100 cm^{-1}) than those computed at the MP2 level. It should be stressed that such a systematic difference is expected since longer N=O bonds are computed with the MP2 method, as has been commented before (see Table 1). All levels of approximations applied here agree with the fact that for both CF_3CH_2SNO and CH_3CH_2SNO molecules, the computed ν(N=O) stretching modes of the *anti* conformations occurs at higher frequencies than those of the *syn* forms. Again,

this is in line with longer bond lenghts computed for the *syn* conformers. The DFT methods yield mean $\Delta\nu$(N=O) = $\nu(N=O)_{anti} - \nu(N=O)_{syn}$ values of 35, 34 and 32 cm^{-1} for CH_3CH_2SNO and 36, 36 and 34 cm^{-1} for CF_3CH_2SNO when the B3P86, B3PW91 and B3LYP functional are used, respectively. For CH_3CH_2SNO a similar value of $\Delta\nu$ = 34 cm^{-1} is found with the MP2 method, but a definite lower difference is obtained for CF_3CH_2SNO with these methods (11 cm^{-1}).

Table 6. Observed and Calculated ν(N=O) (cm^{-1}) for CH_3CH_2SNO and CF_3CH_2SNO

		CH_3CH_2SNO			CF_3CH_2SNO		
		syn	***anti***	**$\Delta\nu$(cm^{-1})**	***syn***	***anti***	**$\Delta\nu$(cm^{-1})**
B3P86	**6-311+G(2df)**	1640	1673	33	1683	1717	34
	cc-pVTZ	1659	1696	37	1698	1736	39
B3PW91	**6-311+G(2df)**	1643	1674	31	1685	1719	34
	cc-pVTZ	1662	1697	35	1700	1738	38
B3LYP	**6-311+G(2df)**	1620	1652	32	1668	1700	32
	cc-pVTZ	1659	1676	17	1685	1721	36
MP2(full)	**6-311+G(2df)**	1443	1480	37	1536	1544	8
	cc-pVTZ	1492	1524	32	1572	1586	14
Experimental		1537	1559	22	1580	1605	25

5-Acknowledgments

The authors are grateful to Deutsche Forschungsgemeinschaft for support through an international project. The Argentinean authors thank the Consejo Nacional de Investigaciones Científicas y Técnicas (CONICET), the Agencia Nacional de

Promoción Científica y Tecnológica and the Facultad de Ciencias Exactas, Universidad Nacional de La Plata for financial support.

6- Supplementary data. The internal and symmetry coordinates used to perform the normal coordinate analysis are defined in Figure S1 and Table S1, respectively. Tables S2 and S3 give thermodynamic and geometrical data computed with 6-31G(d) and 6-311+G(d) basis sets. This material is available free of charge via the Internet at http://pubs.acs.org.

7- References

(1) Tasker, H. S.; Jones, H. O. Action of Mercaptans on Acid Chlorides II. Acid Chlorides of Phosphorus, Sulphur and Nitrogen. *J. Chem. Soc.* **1909**, *95*, 1910-1918.

(2) Petit, C.; Hoffmann, P.; Souchard, J.-P.; Labidalle, S. Synthesis and Characterization of New Aromatic Thionitrites. *Phosphorus, Sulfur Silicon Rel. Elem.* **1997**, *129*, 59-67.

(3) Zolfigol, M. A. Silica Sulfuric Acid/$NaNO_2$ as a Novel Heterogeneous System for Production of Thionitrites and Disulfides under Mild Conditions. *Tetrahedron* **2001**, *57*, 9509-9511.

(4) Soulère, L.; Sturm, J.-C.; Núñez-Vergara, L. J.; Hoffmann, P.; Périé, J. Synthesis, Electrochemical, and Spectroscopic Studies of Novel S-nitrosothiols. *Tetrahedron* **2001**, *57*, 7173-7180.

(5) Williams, D. L. H. The Chemistry of S-Nitrosothiols. *Acc. Chem. Res.* **1999**, *32*, 869-876.

(6) Stamler, J. S.; Toone, E. J. The Decomposition of Thionitrites. *Curr. Opinion Chem. Biol.* **2002**, *6*, 779-785.

(7) Bartberger, M. D.; Mannion, J. D.; Powell, S. C.; Stamler, J. S.; Houk, K. N.; Toone, E. J. S-N Dissociation Energies of S-Nitrosothiols: On the Origins of Nitrosothiol Decomposition Rates. *J. Am. Chem. Soc.* **2001**, *123*, 8868-8869.

(8) Stamler, J. S.; Jaraki, O.; Osborne, J.; Simon, D. I.; Keaney, J.; Vita, J.; Singel, D.; Valeri, C. R.; Loscalzo, J. Nitric Oxide Circulates in Mammalian Plasma Primarily as an S-nitroso Adduct of Serum Albumin. *PNAS* **1992**, *89*, 7674-7677.

(9) Zhang, S.; Çelebi-Ölçüm, N.; Melzer, M. M.; Houk, K. N.; Warren, T. H. Copper(I) Nitrosyls from Reaction of Copper(II) Thiolates with S-Nitrosothiols: Mechanism of NO Release from RSNOs at Cu. *J. Am. Chem. Soc.* **2013**, *135*, 16746-16749.

(10) Schmaunz, A.; Kensy, U.; Slenczka, A.; Dick, B. Photolysis of tert-Butylthionitrite via Excitation to the S1 and S2 States Studied by 3d-REMPI Spectroscopy. *J. Phys. Chem. A* **2010**, *114*, 9948-9962.

(11) Timerghazin, Q. K.; Talipov, M. R. Unprecedented External Electric Field Effects on S-Nitrosothiols: Possible Mechanism of Biological Regulation? *J. Phys. Chem. Lett.* **2013**, *4*, 1034-1038.

(12) Lanucara, F.; Chiavarino, B.; Crestoni, M. E.; Scuderi, D.; Sinha, R. K.; Maître, P.; Fornarini, S. S-nitrosation of Cysteine as Evidenced by IRMPD Spectroscopy. *Int. J. Mass Spectrom.* **2012**, *330-332*, 160-167.

(13) Timerghazin, Q. K.; Peslherbe, G. H.; English, A. M. Structure and Stability of HSNO, the Simplest S-nitrosothiol. *Phys. Chem. Chem. Phys.* **2008**, *10*, 1532-1539.

(14) Fernández-González, M. Á.; Marazzi, M.; López-Delgado, A.; Zapata, F.; García-Iriepa, C.; Rivero, D.; Castaño, O.; Temprado, M.; Frutos, L. M. Structural Substituent Effect in the Excitation Energy of a Chromophore: Quantitative Determination and Application to S-Nitrosothiols. *J. Chem. Theory Comput.* **2012**, *8*, 3293-3302.

(15) Field, L.; Dilts, R. V.; Ravichandran, R.; Lenhert, P. G.; Carnahan, G. E. An Unusually Stable Thionitrite from N-Acetyl-D,L-penicillamine; X-ray Crystal and Molecular Structure of 2-(Acetylamino)-2-carboxy-1,1-Dimethylethyl Thionitrite. *J. Chem. Soc., Chem. Commun.* **1978**, 249-250.

(16) Carnahan, G. E.; Lenhert, P. G.; Ravichandran, R. S-Nitroso-N-acetyl-dl-penicillamine. *Acta Crystallogr.* **1978**, *B34*, 2645-2648.

(17) Arulsamy, N.; Bohle, D. S.; Butt, J. A.; Irvine, G. J.; Jordan, P. A.; Sagan, E. Interrelationships between Conformational Dynamics and the Redox Chemistry of S-Nitrosothiols. *J. Am. Chem. Soc.* **1999**, *121*, 7115-7123.

(18) Bartberger, M. D.; Houk, K. N.; Powell, S. C.; Mannion, J. D.; Lo, K. Y.; Stamler, J. S.; Toone, E. J. Theory, Spectroscopy, and Crystallographic Analysis of S-Nitrosothiols: Conformational Distribution Dictates Spectroscopic Behavior. *J. Am. Chem. Soc.* **2000**, *122*, 5889-5890.

(19) Yi, J.; Khan, M. A.; Lee, J.; Richter-Addo, G. B. The Solid-State Molecular Structure of the S-nitroso Derivative of L-Cysteine Ethyl Ester Hydrochloride. *Nitric Oxide* **2005**, *12*, 261-266.

(20) Goto, K.; Hino, Y.; Kawashima, T.; Kaminaga, M.; Yano, E.; Yamamoto, G.; Takagi, N.; Nagase, S. Synthesis and Crystal Structure of a Stable S-nitrosothiol Bearing a Novel Steric Protection Group and of the Corresponding S-nitrothiol. *Tetrahedron Lett.* **2000**, *41*, 8479-8483.

(21) Perissinotti, L. L.; Estrin, D. A.; Leitus, G.; Doctorovich, F. A Surprisingly Stable S-Nitrosothiol Complex. *J. Am. Chem. Soc.* **2006**, *128*, 2512-2513.

(22) Marazzi, M.; López-Delgado, A.; Fernández-González, M. A.; Castaño, O.; Frutos, L. M.; Temprado, M. Modulating Nitric Oxide Release by S-Nitrosothiol Photocleavage: Mechanism and Substituent Effects. *J. Phys. Chem. A* **2012**, *116*, 7039-7049.

(23) Romano, R. M.; Della Védova, C. O.; Boese, R. A Solid State Study of the Configuration and Conformation of O=S=N-R (R=C_6H_5 and $C_6H_3(CH_3\text{-}CH_2)_2$-2,6). *J. Mol. Struct.* **1999**, *475*, 1-4.

(24) Timerghazin, Q. K.; English, A. M.; Peslherbe, G. H. On the Multireference Character of S-nitrosothiols: A -Theoretical Study of HSNO. *Chem. Phys. Lett.* **2008**, *454*, 24-29.

(25) Hochlaf, M.; Linguerri, R.; Francisco, J. S. On the Role of the Simplest S-nitrosothiol, HSNO, in Atmospheric and Biological Processes. *J. Chem. Phys.* **2013**, *139*, 234304-234308.

(26) Philippe, R. J. The Infrared Spectrum of Methyl Thionitrite. *J. Mol. Spectrosc.* **1961**, *6*, 492-496.

(27) Byler, D. M.; Susi, H. Vibrational Spectra and Normal Coordinate Analysis of Methyl Thionitrite and Isotopic Analogs. *J. Mol. Struct.* **1981**, *77*, 25-36.

(28) Niki, H.; Maker, P. D.; Savage, C. M.; Breitenbach, L. P. Spectroscopic and Photochemical Properties of Methyl Thionitrite (CH_3SNO). *J. Phys. Chem.* **1983**, *87*, 7-9.

(29) Christensen, D. H.; Rastrup-Andersen, N.; Jones, D.; Klabof, P.; Lippincott, E. R. Infrared, Raman and Proton Magnetic Resonance Spectra of Methylthionitrite. *Spectrochim. Acta* **1968**, *A24*, 1581-1589.

(30) Mueller, R. P.; Huber, J. R. Two Rotational Isomers of Methyl Thionitrite: Light-Induced, Reversible Isomerization in an Argon Matrix. *J. Phys. Chem.* **1984**, *88*, 1605-1608.

(31) Kennedy, G. R.; Ning, C. L.; Pfab, J. The 355 nm Photodissociation of Jet-Cooled CH_3SNO: Alignment of the NO Photofragment. *Chem. Phys. Lett.* **1998**, *292*, 161-166.

(32) Banus, J. Perfluoroalkyl Nitroso Compounds. *Nature* **1953**, *171*, 173-174.

(33) Singh, R. P.; Shreeve, J. M. Perfluoroalkylation of Simple Inorganic Molecules: A One Step Route to Novel Perfluoroalkylated Compounds. *Chem. Comm.* **2002**, 1818-1819.

(34) Mason, J. B. Trifluoromethyl Thionitrite. *J. Chem. Soc. (A)* **1969**, 1587-1592.

(35) Kirsch, P.; Bremer, M. Understanding Fluorine Effects in Liquid Crystals. *ChemPhysChem* **2010**, *11*, 357-360.

(36) Oae, S.; Kim, Y. H.; Fukushima, D.; Shinhama, K. New Syntheses of Thionitrites and their Chemical Reactivities. *J. Chem. Soc. Perkin Trans. 1* **1978**, 913-917.

(37) Philippe, R. J.; Moore, H. The Infrared Spectra of Some Alkyl Thionitrites. *Spectrochimica Acta* **1961**, *17*, 1004-1015.

(38) Tilden, W. A. XXXII.-On Aqua Regia and the Nitrosyl Chlorides. *J. Chem. Soc.* **1874**, *27*, 630-636.

(39) Roy, B.; du Moulinet d'Hardemare, A.; Fontecave, M. New Thionitrites: Synthesis, Stability, and Nitric Oxide Generation. *J. Org. Chem.* **1994**, *59*, 7019-7026.

(40) Hibbert, T. G.; Mahon, M. F.; Molloy, K. C.; Price, L. S.; Parkin, I. P. Deposition of Tin Sulfide Thin Films From Novel, Volatile (Fluoroalkythiolato)tin(iv) Precursors. *J. Mat. Chem.* **2001**, *11*, 469-473.

(41) Frisch, M. J.; Trucks, G. W.; Schlegel, H. B.; Scuseria, G. E.; Robb, M. A.; Cheeseman, J. R.; Montgomery Jr., J. A.; Vreven, T.; Kudin, K. N.; Burant, J. C.; *et al.* Gaussian 03; Revision B.04 ed.; Gaussian, Inc.: Pittsburgh PA, 2003.

(42) Perdew, J. P. Density-Functional Approximation for the Correlation Energy of the Inhomogeneous Electron Gas. *Phys. Rev. B* **1986**, *33*, 8822-8824.

(43) Lee, C.; Yang, W.; Parr, R. G. Development of the Colle-Salvetti Correlation-Energy Formula into a Functional of the Electron Density. *Phys. Rev. B* **1988**, *37*, 785-789.

(44) Becke, A. D. Density-Functional Thermochemistry. III. The Role of Exact Exchange. *J. Chem. Phys.* **1993**, *98*, 5648-5652.

(45) Hedberg, L.; Mills, I. M. Harmonic Force Fields from Scaled SCF Calculations: Program ASYM40. *J. Mol. Spectrosc.* **2000**, *203*, 82-95.

(46) Baciu, C.; Gauld, J. W. An Assessment of Theoretical Methods for the Calculation of Accurate Structures and SN Bond Dissociation Energies of S-Nitrosothiols (RSNOs). *J. Phys. Chem. A* **2003**, *107*, 9946-9952.

(47) Fu, Y.; Mou, Y.; Lin; Liu, L.; Guo, Q.-X. Structures of the X-NO Molecules and Homolytic Dissociation Energies of the Y-NO Bonds (Y = C, N, O, S). *J. Phys. Chem. A* **2002**, *106*, 12386-12392.

(48) Erben, M. F.; Della Védova, C. O.; Romano, R. M.; Boese, R.; Oberhammer, H.; Willner, H.; Sala, O. Anomeric and Mesomeric Effects in Methoxycarbonylsulfenyl Chloride, $CH_3OC(O)SCl$: An Experimental and Theoretical Study. *Inorg. Chem.* **2002**, *41*, 1064-1071.

(49) Pasinszki, T.; Vass, G. b.; Klapstein, D.; Westwood, N. P. C. Generation, Spectroscopy, and Structure of Cyanoformyl Chloride and Cyanoformyl Bromide, XC(O)CN. *J. Phys. Chem. A* **2012**, *116*, 3396-3403.

(50) Erben, M. F.; Della Védova, C. O.; Boese, R.; Willner, H.; Oberhammer, H. Trifluoromethyl Chloroformate, $ClC(O)OCF_3$: Structure, Conformation, and Vibrational Analysis Studied by Experimental and Theoretical Methods. *J. Phys. Chem. A* **2004**, *108*, 699-706.

(51) Seth-Paul, W. A. Classical and Modern Procedures for Calculating PR Separations of Symmetrical and Asymmetrical Top Molecules. *J. Mol. Struct.* **1969**, *3*, 403-417.

TOC Graphic